

Figure S1. **Alignment and phylogeny for SKAP and its isoforms and characterization of SKAP isoforms in mouse cells and tissues.** (A, top) IP-mass spectrometry data using an antibody to the long form of mouse SKAP from mouse testes analyzed for Astrin and SKAP peptides. (bottom) Identified SKAP peptides mapped against SKAP aa sequence (ID: Q9Y448-1). (B) Alignment of human versus mouse SKAP proteins using Jalview software. Identity is shown in blue. The N-terminal testis extension is boxed in black, and the start of the mitotic isoform is marked with an arrow. The SX[I/L]P motif in each protein is boxed in red. (C) Phylogeny for SKAP derived from TimeTree species divergence data. Astrin and the short (mitotic) form of SKAP are first visible in vertebrates. The long (testis-specific) isoform is first detectable in placental (eutherian) mammals (highlighted in yellow). (D) Western blot showing the presence of the SKAP long and short isoforms in the indicated cells and tissues. The short form is present in mitotic cells and tissues. The long (testis-specific) form appears in adult mouse testis. Tubulin is shown as a relative control for loading levels. Tubulin displays a shift in its mobility because of its increasing posttranslational modification state, from left to right. *, nonspecific bands. (E) IF of the human full-length SKAP antibody in a metaphase mouse 3T3 cell. The image represents a maximum-intensity projection. SKAP localizes to kinetochores and the mitotic spindle. Bar, 5 μ m. (F) Testis section visualized for SKAP using an immunohistochemical stain imaged with a bright field microscope using a 100 \times objective. (left) Image of a region of a mouse tubule with lumen and elongating spermatids indicated. (right) Zoom of a meiotic cell showing SKAP spindle staining. Bar, 20 μ m.

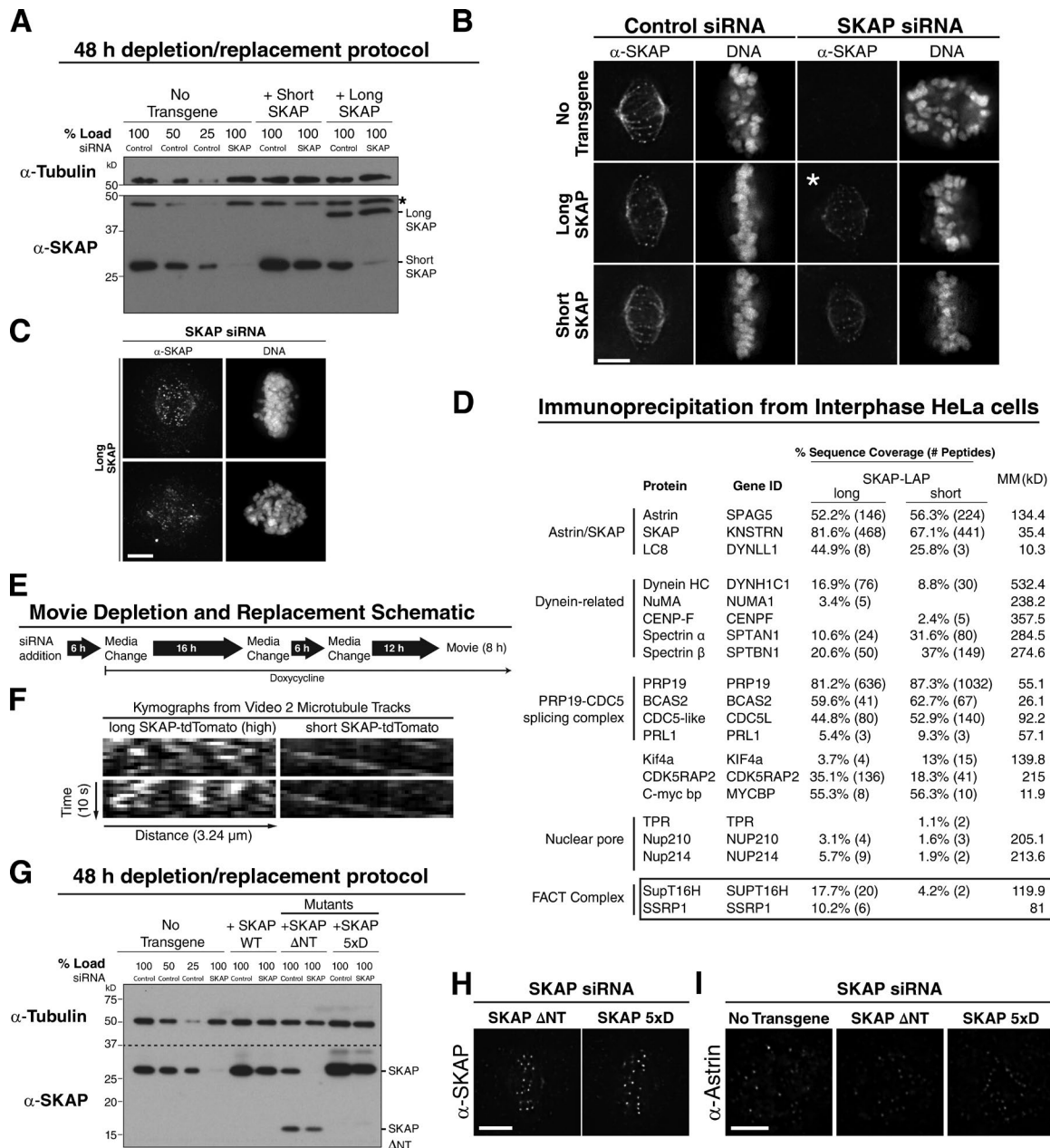


Figure S2. **SKAP interphase interactions and validation of the SKAP depletion and replacement protocols.** (A) Western blot for the 48-h depletion and SKAP replacement protocol. Tubulin was used as a loading control. The membrane was cut to probe with the SKAP and tubulin antibodies as indicated. *, nonspecific band. (B) SKAP IF for SKAP depletion and rescue experiments. (*) This cell with aligned chromosomes was rare in this condition but is included to show SKAP localization to aligned kinetochores and the slight reduction in spindle localization. For localization representing the spindle morphology in the majority of cells in this condition, see C. (C) IF showing SKAP localization in cells in which the long SKAP isoform replaces endogenous SKAP. These images are included to highlight SKAP localization in cells with misaligned chromosomes, which are more typical of this condition and are scaled separately for visibility. (D) Interphase interactions for SKAP-LAP showing the mass spectrometry sequence coverage obtained for affinity purifications of the long and short forms. LAP-preps were performed using the same reagents on the same day, and 300 mM KCl was used in buffers for both bead binding and washing. (E) Schematic showing protocol for phenotype videos. (F) Kymographs showing the behavior of the indicated SKAP constructs on microtubules in interphase cells, generated from microtubule tracks from Video 2. (left) Long SKAP-tdTomato displaying microtubule interactions and diffusion, but not plus-end tracking behavior. (right) Short SKAP-tdTomato showing plus-end tracking along a growing microtubule. (G) Western blot for the 48-h depletion and SKAP replacement protocol for SKAP microtubule-binding mutants. The membrane was cut as indicated by dotted line to probe with the different antibodies. (H) IF images showing SKAP and DNA localization in the indicated SKAP microtubule-binding mutants for rare cells with aligned metaphase plates. (I) IF images showing Astrin localization in the indicated conditions in cells with misaligned chromosomes. Bars, 5 μ m.

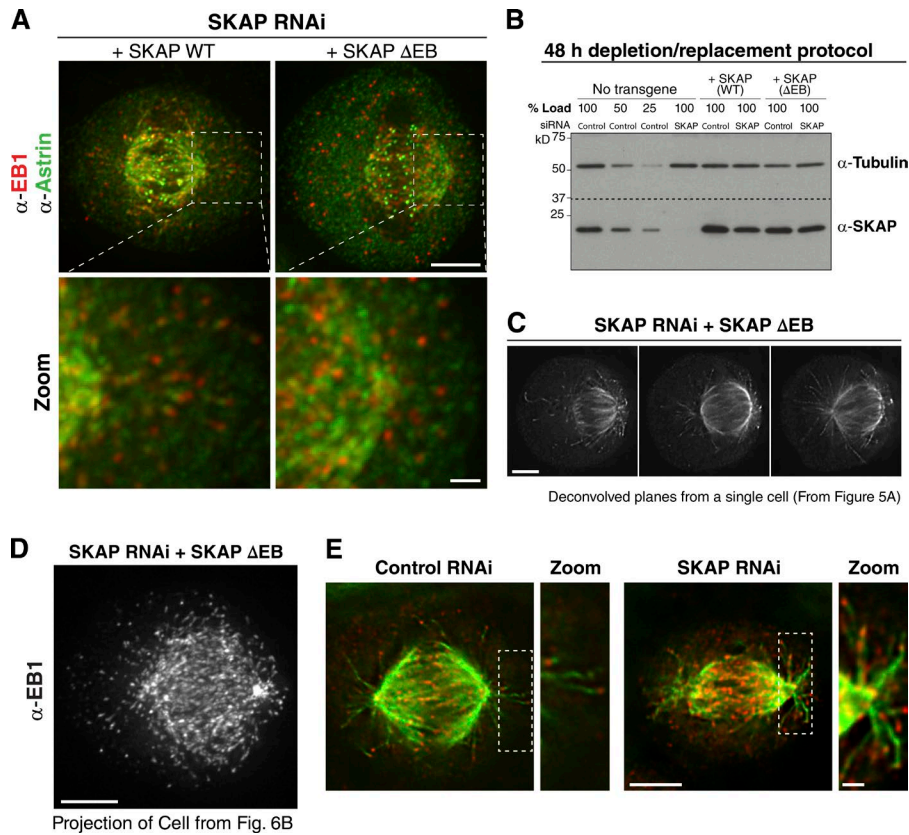


Figure S3. **SKAP mitotic plus-end tracking, validation of the SKAP depletion and SKAP Δ EB mutant replacement protocol, spindle positioning experiment controls, and astral microtubule phenotype.** (A, top) IF of EB1 and Astrin from SKAP wild-type (WT) and SKAP Δ EB cells. (bottom) Zoom of a region near the centrosome showing Astrin plus-end tracking. (B) Western blot for the 48-h depletion and SKAP replacement protocol for the SKAP Δ EB mutant. Tubulin was used as a loading control. The membrane was cut as indicated by dotted line to probe with each antibody. (C) Deconvolved planes from shifted cell depicted in Fig. 5 A. (D) Maximum-intensity projection for the cell from Fig. 6 B showing the extent of growing microtubule ends along cortex on the right side of the cell and the relative lack of microtubule contact with cortex on the left. (E) IF images (deconvolved planes) showing microtubule and rabbit anti-EB1 localization for control and SKAP-depleted cells. Boxed regions are enlarged on right ($\sim 2\times$) to show plus ends of microtubules growing laterally along the cortex. Images in this panel are scaled individually for clarity. Bars: 5 μ m; (inset/zoom) 1 μ m.

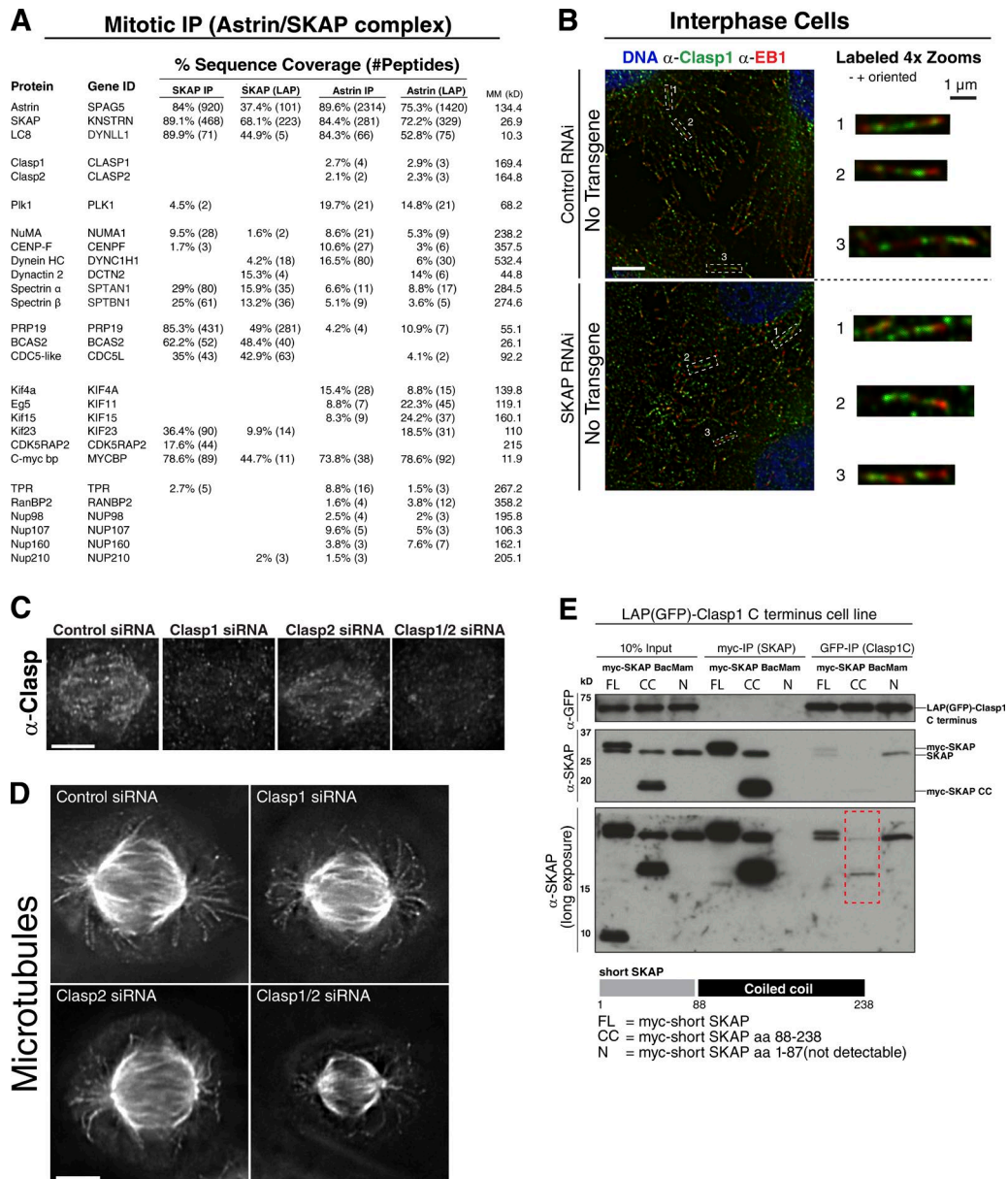
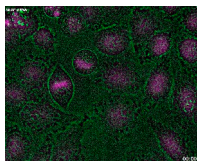
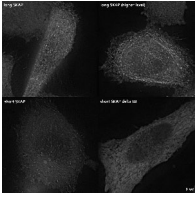


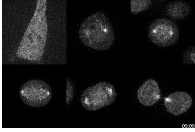
Figure S4. **Mitotic interactions of the Astrin/SKAP complex and interphase Clasp1 localization.** (A) IP-mass spectrometry of Astrin and SKAP, including GFP-tagged protein IP and direct antibody IP. For these purifications, the following concentrations of KCl were included in the wash buffer: SKAP antibody IP from HeLa cells (300 mM KCl), SKAP-LAP (100 and 300 mM KCl preparations), Astrin antibody IP from HeLa cells (300 mM KCl), LAP-Astrin IP (two purifications from Schmidt et al. [2010] at 300 mM KCl; one from this study conducted with 100 mM KCl), LAP-Astrin (aa 458–1,193) IP with 300 mM KCl, and a Flp-In Astrin-LAP IP with 200 mM KCl in which Astrin-LAP was induced with 1 μ g/ml doxycycline for 16 h and the cells were arrested in mitosis with 10 μ M STLC. All other preparations are from nocodazole-arrested cells. Only proteins with peptides identified in at least two of types of preparation or in the interphase SKAP IPs are depicted here. Proteins that are commonly seen across many unrelated preparations were excluded. MM, molecular mass. (B) Interphase localization of Clasp1 to microtubules and plus ends. The boxed region on the left is presented as a zoomed-in image on the right. (C) IF images showing localization of the Clasp antibody in Clasp depletion conditions. (D) IF images showing spindle architecture in Clasp depletions. Each image is scaled individually, and the gamma was adjusted to visualize astral microtubules clearly. (E) IP followed by Western blot using the GFP-Clasp1 C terminus cell line and BacMam-expressed, myc-tagged SKAP constructs as indicated. The red boxed area shows the immunoprecipitation of the overexpressed SKAP coiled coil by Clasp1 C terminus. Bars: 5 μ m; (zoom) 1 μ m.



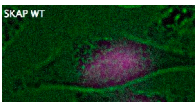
Video 1. **SKAP depletion causes multiple mitotic defects.** Cells going through mitosis with SKAP depletion (related to Fig. 2). DNA, magenta; differential interference contrast microscopy, green. Total imaging time: 8 h.



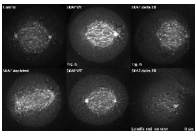
Video 2. **Interphase expression of long versus short SKAP-tdTomato constructs.** Cells in interphase with indicated transfected constructs (related to Fig. 2). Expression of long SKAP leads to puncta in interphase and weak microtubule localization. However, short SKAP displays clear plus-end tracking. Videos are scaled identically.



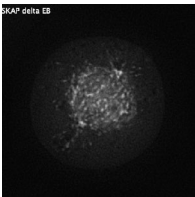
Video 3. **SKAP tracks microtubule plus ends.** SKAP-GFP on a spinning disc confocal microscope (see Materials and methods; related to Fig. 4). Total imaging time: 30 s.



Video 4. **SKAP Δ EB cells display a spindle shift in metaphase.** Mitotic cells used for kymographs in Fig. 5 D. SKAP wild-type (WT; left) and Δ EB cells are shown. Total time: 70 min.



Video 5. **Astral microtubule plus ends grow laterally along the cell cortex in metaphase SKAP Δ EB cells.** Examples of EB3-tdTomato videos for control, SKAP-depleted, rescued, and SKAP Δ EB cells including the two displayed in Fig. 6 D as indicated. Total imaging time 60 s; 30 s for SKAP wild type (WT). Images collected every 2 s. All videos are scaled equivalently.



Video 6. **Additional metaphase SKAP Δ EB cell videos.** Additional videos showing EB3-marked plus ends in SKAP Δ EB cells (related to Fig. 6 and Video 5).

Table S1. Cell lines used in this study

Cell line	Type	Used	Source
HeLa	HeLa	Fig. 1 A, direct antibody IPs	NA
NIH/3T3	Mouse embryonic fibroblast	Fig. S1	NA
HeLa Flp-In	HeLa Flp-In	No transgene control, generation of Flp-In cell lines	Stephen Taylor Lab
Long SKAP-LAP	HeLa retroviral clonal line	Fig. 2	This study
Short SKAP-LAP	HeLa retroviral clonal line	Figs. 2, 3, and 4, Video 3, and IP mass spectrometry	This study
Short SKAP Δ NT-LAP (aa 89–238)	HeLa retroviral clonal line	Fig. 3	This study
Short SKAP 5xD-LAP	HeLa retroviral clonal line	Fig. 3	This study
Short SKAP Δ EB-LAP	HeLa retroviral clonal line	Fig. 4	This study
LAP-Astrin	HeLa retroviral clonal line	LAP-Astrin IP mass spectrometry	Schmidt et al., 2010
LAP-Astrin (aa 458–1,193)	HeLa retroviral clonal line	LAP-Astrin IP mass spectrometry	This study
LAP-Clasp1 (aa 1,258–1,538)	HeLa retroviral clonal line	Fig. 7	This study
Flp-In long SKAP	HeLa Flp-In IRES eGFP	Fig. 2	This study
Flp-In short SKAP	HeLa Flp-In IRES eGFP	Replacement and rescue experiments	This study
Flp-In short SKAP Δ NT (aa 89–238)	HeLa Flp-In IRES eGFP	Fig. 3	This study
Flp-In short SKAP 5xD	HeLa Flp-In IRES eGFP	Fig. 3	This study
Flp-In short SKAP Δ EB	HeLa Flp-In IRES eGFP	Replacement experiments	This study
Flp-In Astrin-LAP	HeLa Flp-In C-term LAP	Astrin-LAP IP mass spectrometry	This study

All SKAP cell lines are RNAi resistant. Retroviral cell lines were selected and maintained using blasticidin. HeLa Flp-In parental line was maintained in zeocin and blasticidin. Flp-In lines were selected and maintained using blasticidin and hygromycin. NA, not applicable.

Reference

Schmidt, J.C., T. Kiyomitsu, T. Hori, C.B. Backer, T. Fukagawa, and I.M. Cheeseman. 2010. Aurora B kinase controls the targeting of the Astrin-SKAP complex to bioriented kinetochores. *J. Cell Biol.* 191:269–280. <http://dx.doi.org/10.1083/jcb.201006129>